A Coupled Numerical Technique for Self-Consistent Analysis of Micro-Electro-Mechanical-Systems

N. R. Aluru and J. White
Department of Electrical Engineering and Computer Science
Massachusetts Institute of Technology, Cambridge, MA 02139

ABSTRACT

An efficient algorithm for self-consistent analysis of 3-D micro-electro-mechanical-systems (MEMS) is described. The algorithm employs a hybrid finite-element/boundary-element technique for coupled mechanical and electrical analysis. The coupled algorithm is shown to converge rapidly and is much faster than relaxation for tightly coupled problems.

I. INTRODUCTION

In order to investigate design alternatives, designers of novel MEMS structures need efficient, robust and easily used computer simulation tools. And since most of the structures of interest are geometrically complicated, electromechanically coupled, and are inherently three-dimensional, Micro-Electro-Mechanical CAD (MEMCAD) tool developers have been focussed on improving the usability, efficiency and robustness of coupled 3-D electro-mechanical analysis. The behavior of micro-electro-mechanical devices can be predicted by the solution of coupled problems involving mechanical or elastostatic analysis and electrical or electrostatic analysis. The numerical techniques employed for coupled electro-mechanical analysis have so far been based on relaxation [5], [6] and a form of surface-Newton method [2], [19]. In particular, finite-element based elastostatic analysis and accelerated boundary-element based electrostatic analysis have been combined using algorithms based on relaxation and a form of surface-Newton method. The relaxation algorithm is easy to program, only requiring that data be passed back and forth between "black-box" elastostatic (e.g. ABAQUS [10]) and electrostatic (e.g. FASTCAP [13]) analysis programs. However, the algorithm diverges if the structure is too flexible or the electric fields are too large [19]. Matrix-free surface-Newton methods preserve the "black-box" nature of the relaxation algorithm and have better convergence properties, but also have perturbation parameters which must be tuned for good performance. In addition, each surface-Newton iteration requires several nonlinear elastostatic and linear electrostatic analyses. Hence, the surface-Newton approach is not very efficient. In this paper, we present a new technique to improve the efficiency of coupled 3-D electro-mechanical analysis.

This paper is organized as follows: The elastostatic and electrostatic analysis are described in Sections II and III, respectively. A coupled approach to 3-D electro-mechanical analysis is presented in Section IV. Numerical results are presented in Section V and finally conclusions are given in Section VI.

II. ELASTOSTATICS

Micro-mechanical structures undergo large deformation when subjected to electrostatic actuation. The nonlinear structural deformation can be determined by considering the equilibrium of the body in the deformed configuration. Since the deformed structural configuration is not known, the equilibrium equations can be transformed and expressed with reference to either the original undeformed, unstressed configuration or to the last computed deformed configuration. The first approach, where the equilibrium equations are expressed with reference to the original configuration, is defined as the total Lagrangian (or simply Lagrangian) technique and the second approach is defined as the updated Lagrangian technique (see e.g. [3] for differences between the two approaches). A key issue with either approach is the appropriate definition of stress and strain measures. In a Lagrangian approach, the technique employed in this paper, the appropriate stress and strain measures are, respectively, the 2nd Piola-Kirchoff stress tensor and the Green-Lagrange strain tensor [12].

Denoting Ω to be the initial configuration occupied by a material body and Γ to be the material boundary, the nonlinear equilibrium equations for finite deformation of a structure, expressed with reference to the initial configuration, are summarized as follows [12]:

$$\nabla \bullet (\nabla\varphi S) + \rho_0 f = 0 \; in \; \Omega \quad (1)$$

$$\varphi = g \; on \; \Gamma_g \quad (2)$$

$$F_{iA} S_{AB} N_B = h_i \; on \; \Gamma_{h_i} \quad (3)$$

where $F = \nabla\varphi$ is the deformation gradient matrix, φ is the transformation which maps points from the original configuration X to the deformed configuration x i.e $x = \varphi(X)$, S is the symmetric Piola-Kirchoff stress tensor, ρ_0 is the density of the material, f is the body force, g are the Dirichlet boundary conditions specified on the boundary Γ_g, the tractions h_i are the natural boundary conditions specified on the boundary Γ_{h_i}, $F_{iA} = \partial\varphi_i/\partial X_A$, S_{AB}, $1 \leq i, A, B \leq 3$ denote the components of the deformation gradient and stress tensor, respectively, and N_B is the unit outward normal.

The transformation $\varphi(X)$ can be written as

$$x = \varphi(X) = X + u \quad (4)$$

where u is the unknown displacement vector. The stress components, S_{AB}, are related to the strain components, E_{AB}, by the constitutive equation

$$S_{AB} = \frac{\partial W(E)}{\partial E_{AB}} \quad (5)$$

where $W(E_{AB}(\varphi))$ is the stored energy function of the material. The strain components are related to φ by the relation

$$E_{AB} = \frac{1}{2}\left[\frac{\partial\varphi_i}{\partial X_A}\frac{\partial\varphi_i}{\partial X_B} - \delta_{AB}\right] \quad (6)$$

where δ_{AB} is the Kronecker delta.

Equations (1)–(6) summarize the fundamental nonlinear elastostatic model for finite deformation of a structure. The coupling to the electrostatic equations appears through the surface tractions. The surface charges create an electrostatic pressure that acts in the direction of the structure surface normal. The electrostatic pressure is given by the expression

$$h = \frac{1}{2} E_n * \sigma \quad (7)$$

where σ is the surface charge density, determined through a solution of the electrostatic equations, and E_n is the normal electric field at the surface.

This research was supported by ARPA under ONR contract DABT63-94-C-0053 and FBI contract J-FBI-92-196, by SRC under contract SJ-558, and by grants from IBM and Digital Equipment Corporation.

A. Finite Element Formulation

The nonlinear elastostatic equations are discretized by employing a Galerkin finite element method. Denote η to be a test function and let the variational functional spaces $\mathcal{S}$ and $\mathcal{V}$ consist of continuous functions with square integrable first derivatives. The solution space $\mathcal{S}$ is the set of all such functions satisfying the Dirichlet boundary conditions. The weighting or test function space $\mathcal{V}$ is made up of functions whose value is zero where Dirichlet boundary conditions are specified i.e.

$$\{\mathcal{S} = u \mid u \in H^1, u = g - X \; on \; \Gamma_g\} \quad (8)$$

$$\{\mathcal{V} = \eta \mid \eta \in H^1, \eta = 0 \; on \; \Gamma_g\} \quad (9)$$

The weak-form of elastostatics is then stated as follows: Given ρ_0, f, g and h_i, find $u \in \mathcal{S}$ such that for all $\eta \in \mathcal{V}$

$$\int_\Omega \nabla\eta : \left[\nabla\varphi S(E(\varphi))\right] d\Omega - \int_\Omega \rho_0 f \eta d\Omega - \int_{\Gamma_h} \eta h d\Gamma = 0 \quad (10)$$

Let $\mathcal{S}^h \subset \mathcal{S}$ and $\mathcal{V}^h \subset \mathcal{V}$ be finite dimensional approximations to $\mathcal{S}$ and $\mathcal{V}$ respectively. The Galerkin form is then stated as follows: Given ρ_0, f, g and h_i, find $u^h \in \mathcal{S}^h$ such that for all $\eta^h \in \mathcal{V}^h$

$$\int_\Omega \nabla\eta^h : \left[\nabla\varphi^h S^h(E^h(\varphi^h))\right] d\Omega - \int_\Omega \rho_0 f \eta^h d\Omega - \int_{\Gamma_h} \eta^h h d\Gamma = 0 \quad (11)$$

To construct a matrix form, the trial and test functions are approximated by linear basis functions i.e.

$$u^h = \sum_{a=1}^{nnd} N_a \, d_a \quad (12)$$

$$\eta^h = \sum_{a=1}^{nnd} N_a \, c_a \quad (13)$$

where nnd is the number of finite element nodes, N_a is the shape function of node a, d_a is the unknown displacement vector of node a, and c_a is the arbitrary weighting function vector. Substitution of (12) and (13) into the Galerkin form (11) leads to a nonlinear system of equations which is linearized and solved incrementally for the displacement u. The nonlinear residual equation for a finite element node, a, is given as

$$R_a = \int_\Omega \mathcal{B}_a^T \hat{S} \, d\Omega - \int_\Omega N_a \rho_0 f \, d\Omega - \int_{\Gamma_h} N_a h \, d\Gamma \quad (14)$$

where

$$\mathcal{B}_a = \begin{bmatrix} [\varphi^h_{,1}]^T N_{a,1} \\ [\varphi^h_{,2}]^T N_{a,2} \\ [\varphi^h_{,3}]^T N_{a,3} \\ [\varphi^h_{,1}]^T N_{a,2} + [\varphi^h_{,2}]^T N_{a,1} \\ [\varphi^h_{,2}]^T N_{a,3} + [\varphi^h_{,3}]^T N_{a,2} \\ [\varphi^h_{,1}]^T N_{a,3} + [\varphi^h_{,3}]^T N_{a,1} \end{bmatrix} \quad \hat{S} = \begin{bmatrix} S_{11} \\ S_{22} \\ S_{33} \\ S_{12} \\ S_{23} \\ S_{31} \end{bmatrix} \quad (15)$$

$\varphi_{,i}$ denotes differentiation with respect to the ith coordinate and S_{ij} is the i, jth component of the stress tensor.

III. Electrostatics

In electrostatic analysis, the conductor potentials are specified and the potential must satisfy the Laplace's equation in the region between the conductors. The charge on each conductor can be determined by solving the integral equation [16]

$$\psi(x) = \int_{surfaces} \sigma(x') \frac{1}{4\pi\epsilon_0 \|x - x'\|} da', \quad x \in surfaces \quad (16)$$

where $\psi(x)$ is the known conductor surface potential, σ is the surface charge density, da' is the incremental conductor surface area, x, $x' \in \mathbf{R}^3$, and $\|x\|$ is the usual Euclidean length of x given by $\sqrt{x_1^2 + x_2^2 + x_3^2}$.

A standard approach to numerically solving (16) for σ is to use a piece-wise constant collocation scheme. That is, the conductor surfaces are broken into n small panels, and it is assumed that on each panel i, a charge, q_i, is uniformly distributed. Then for each panel, an equation is written which relates the known potential at the center of that i-th panel, denoted $\overline{p}_i$, to the sum of the contributions to that potential from the n charge distributions on all n panels [15]. The result is a dense linear system,

$$Pq = \overline{p} \quad (17)$$

where $P \in \mathbf{R}^{n \times n}$, q is the vector of panel charges, $\overline{p} \in \mathbf{R}^n$ is the vector of known panel potentials, and

$$P_{ij} = \frac{1}{a_j} \int_{panel_j} \frac{1}{4\pi\epsilon_0 \|x_i - x'\|} da', \quad (18)$$

where x_i is the center of the i-th panel and a_j is the area of the j-th panel.

The dense linear system of (17) can be solved to compute panel charges from a given set of panel potentials. If Gaussian elimination is used to solve (17), the number of operations is order n^3. Clearly, this approach becomes computationally intractable if the number of panels exceeds several hundred. Instead, consider solving the linear system (17) using a conjugate-residual style iterative method like GMRES [17]. Such methods have the form given below:

Algorithm 1: GMRES algorithm for solving (17)
Make an initial guess to the solution, q^0.
Set $k = 0$.
do {
  Compute the residual, $r^k = \overline{p} - Pq^k$.
  if $\|r\| < tol$, return q^k as the solution.
  else {
    Choose α's and β in
      $q^{k+1} = \sum_{j=0}^{k} \alpha_j q^j + \beta r^k$
    to minimize $\|r^{k+1}\|$.
    Set $k = k + 1$.
  }
}

The dominant costs of Algorithm 1 are in calculating the n^2 entries of P using (18) before the iterations begin, and performing n^2 operations to compute Pq^k on each iteration. A precorrected-FFT algorithm which, through the use of carefully applied approximations and transform techniques, avoids forming most of P and reduces the cost of forming Pq^k to order $n \log n$ operations.

A. The Precorrected-FFT Approach

The precorrected-FFT approach generates an implicit approximation to P which can be used to compute the matrix-vector products Pq rapidly [14]. In this approach, the interaction between nearby panels is computed explicitly. These entries in the potential coefficient matrix, P, are computed by employing Equation (18).

In a subsequent step, the portion of the matrix-vector product Pq associated with distant interactions is computed by employing an

FFT algorithm. Specifically, a three-dimensional grid is first constructed to include all the panels. The charge in each panel is then projected onto the grid. The potential at the grid points due to grid charges is a three-dimensional convolution. The convolution can be computed rapidly by employing the FFT algorithm. The grid potentials are then interpolated onto the panels to obtain the potential on each panel. The problem, however, with the FFT approach to compute distant interactions is that the computation of the matrix-vector product for nearby panels is duplicated. In addition, the calculation of the nearby potential by grid approximation is not accurate. Hence, the poor approximation generated by the grid approach to nearby panels is subtracted from the direct interactions. This step is referred to as the precorrection. The matrix-vector product is then obtained by adding the precorrected direct interactions and the grid approximated distant interactions.

IV. Coupled Algorithm

In a coupled approach to 3-D electro-mechanical analysis, the elastostatic and electrostatic equations are solved as a single system. This approach, in comparison to the relaxation algorithm, takes into account the strong coupling between electrical and mechanical systems and in comparison to the surface-Newton technique avoids the several nonlinear elastostatic and linear electrostatic solves during each inner iteration. A coupled approach has been attempted before [18] by employing a finite element method for both the electrostatic and elastostatic equations. This approach may not be computationally very efficient as a finite-element method, in comparison to a precorrected-FFT accelerated boundary-element method, would require the construction of an exterior mesh for the electrostatic analysis. A computationally efficient approach of a hybrid finite-element/boundary-element method is employed in this paper. A coupled algorithm for electro-mechanical analysis is shown in Figure 1. The outer Newton iteration solves the nonlinear coupled system, and the linear system within each Newton iteration is solved using the GMRES algorithm.

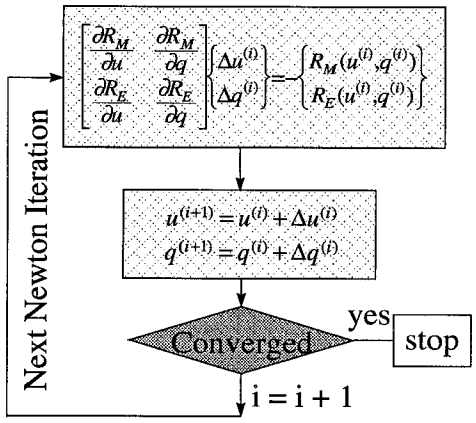

Figure 1. A coupled algorithm for self-consistent electro-mechanical analysis.

A number of issues must be addressed in the coupled approach. First is the efficient computation of the coupled system Jacobian or the matrix-vector product involving the Jacobian and the displacement/charge vector when employing iterative solution techniques. Second is the storage cost for the coupled system Jacobian. Matrix-free techniques can be used to advantage to minimize storage cost. However, the robustness of the matrix-free technique is very sensitive to the precise choice of the perturbation parameter. If the perturbation parameter is too large, the nonlinearities in the residual will corrupt the derivative estimate. If the perturbation parameter is too small, the small numerical errors in solving the electrostatic and elastostatic problems will corrupt the derivative estimate. Third is the definition of appropriate units for the Jacobian and the residual. The variables in the elastostatic and electrostatic equations represent different units and scales and care should be exercised when computing the Jacobian or the residual. This is easily handled by nondimensionalizing both the elastostatic and electrostatic systems. The issues of storage and efficient computation of the Jacobian are discussed in the following paragraphs.

The coupled system Jacobian can be divided into four parts: the entirely elastostatic part, often referred to as the stiffness or the deformation-coefficient matrix, which determines the change in force due to geometric perturbations; the entirely electrostatic part, which determines the change in potential due to perturbations in surface charge; the electrical to mechanical part, which determines the change in force due to perturbation in surface charge; and the mechanical to electrical part, which determines the change in potentials due to geometric perturbations. The deformation-coefficient matrix is computed by employing a Galerkin finite-element formulation as discussed in section II. The formulation accounts for both material and geometric nonlinearities and is summarized in Figure 2(a). A sparse storage scheme [11] is employed to store the deformation-coefficient matrix. The electrostatic or the potential coefficient matrix is not needed explicitly as the GMRES algorithm, within each Newton iteration, requires only a matrix-vector product involving the matrix, $\frac{\partial R_E}{\partial q}$, and the charge increment vector, Δq. This matrix-vector product can be computed by employing the precorrected-FFT algorithm discussed in section III. In earlier approaches to electro-mechanical simulations [5], [6], [19], a multipole algorithm [8] is employed to efficiently compute the matrix-vector product. The precorrected FFT algorithm, as compared to the multipole algorithm, has been shown to be faster and more memory efficient [14]. The computation of the matrix-vector product with the precorrected FFT technique is summarized in Figure 2(b).

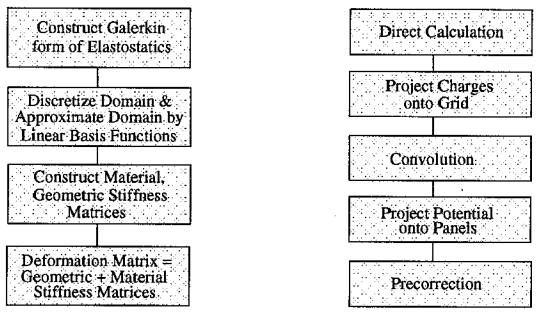

Figure 2. (a) Computation of the deformation coefficient matrix (b) Computation of the matrix-vector product employing precorrected-FFT technique.

A. Electrical to Mechanical Coupling

The electrical to mechanical coupling, $\frac{\partial R_M}{\partial q}$, is obtained from Equation (14) as

$$\frac{\partial R_M^a}{\partial q} = -\int_{\Gamma_h} N_a \frac{\partial h}{\partial q}\, d\Gamma \tag{19}$$

where R_M^a is the residual equation for the finite element node a, and noting that $\sigma = q/A$, where A is the panel area, $\partial h/\partial q$ is obtained

trivially from Equation (7).

The computation in Equation (19) can be performed by computing an equivalent pressure ($\partial h/\partial q$) for each boundary face that belongs to both mechanical and electrical domains. The size of the mechanical to electrical coupling matrix is $3m \times n$ where m is the total number of finite element nodes on the mechanical domain and n is the total number of surface panels on the electrical domain. This coupling matrix is, however, very sparse as each finite element node belongs to only a few panels. Hence, only the non-zero entries of the coupling matrix are stored.

B. Mechanical to Electrical Coupling

The mechanical to electrical coupling term can be computed by employing a matrix-free approach. The residual equation for the electrostatic system is given as

$$R_E = P(u)q - \overline{p} = 0 \tag{20}$$

where $P(u)$ is the displacement dependent potential-coefficient matrix, q is the charge vector and $\overline{p}$ is the vector of applied potentials. An approach to compute the mechanical to electrical coupling term is given as

$$\frac{\partial R_E}{\partial u}\Delta u^{(i)} \approx \frac{P(u + \epsilon\Delta u^{(i)})q - P(u)q}{\epsilon} \tag{21}$$

where ϵ is a small parameter. In order to compute the matrix-vector product, $\frac{\partial R_E}{\partial u}\Delta u^{(i)}$, accurately a small value of ϵ is desired and is determined through an optimization problem [7]. For well-scaled residuals, an optimal value of ϵ is $O(\epsilon_m^{1/2})$, where ϵ_m is the machine precision. Unlike the surface-Newton technique, the choice of the matrix-free parameter, ϵ, is not critical and does not effect the robustness or the accuracy of the coupled algorithm [1].

According to Equation (21), the mechanical to electrical coupling can be computed by performing two matrix-vector products. The first matrix-vector product, $P(u)q$, is straight forward and is computed in the outer Newton loop. The second matrix-vector product, $P(u + \epsilon\Delta u^{(i)})q$, can be obtained by perturbing the panel/conductor geometry from u to $u + \epsilon\Delta u^{(i)}$ and determining the new potential coefficient matrix, $P(u + \epsilon\Delta u^{(i)})$. The second matrix-vector product is computed in the inner GMRES loop by employing the approximations generated by GMRES to $\Delta u^{(i)}$.

The two matrix-vector products required to compute the electrical to mechanical coupling can be obtained by employing either the precorrected FFT technique or a direct method. In a setup phase, the precorrected FFT technique computes all the transformation matrices (precorrected direct interactions, projection of panel charges onto grid, FFT and projection of grid potential onto panels). The transformation matrices are a function of the geometry and need to be computed once. In a subsequent evaluation phase, the matrix-vector product can be computed in order $n \log n$ operations. Clearly, the overhead in the precorrected FFT technique is the setup phase. In order to compute the matrix-vector product, $P(u + \epsilon\Delta u^{(i)})q$, a setup is needed during each iteration of the inner GMRES loop. An additional setup is needed if a preconditioner is to be employed (discussed in the next section). A computationally efficient approach is to employ a direct method i.e. for nearby panels the potential is computed using the exact analytical formulae [9] and the distant panels are evaluated using quadrature rules. The complexity of the direct approach is order $p^2 + 2pq$, where p is the number of panels on the mechanical domain and $p + q = n$. As will be discussed below, a preconditioner can be applied very efficiently with a direct calculation. In either approach, only two vectors of size n need to be stored to compute the mechanical to electrical coupling.

C. Preconditioner

A block diagonal preconditioner of the form

$$\Pi = \begin{bmatrix} R_{Mu}^{-1} & 0 \\ 0 & R_{Eq}^{-1} \end{bmatrix} \tag{22}$$

is applied to the coupled linear system to accelerate the convergence of the GMRES algorithm. In the above equation, Π denotes the preconditioner, $R_{Mu} = \partial R_M/\partial u$ is the deformation coefficient matrix, and $R_{Eq} = \partial R_E/\partial q$ is the potential coefficient matrix. The preconditioned linear system is written as

$$\begin{bmatrix} I & R_{Mu}^{-1}R_{Mq} \\ R_{Eq}^{-1}R_{Eu} & I \end{bmatrix} \begin{Bmatrix} \Delta u^{(i)} \\ \Delta q^{(i)} \end{Bmatrix} = - \begin{Bmatrix} R_{Mu}^{-1}R_M \\ R_{Eq}^{-1}R_E \end{Bmatrix} \tag{23}$$

where $R_{Mq} = \partial R_M/\partial q$ denotes the electrical to mechanical coupling and $R_{Eu} = \partial R_E/\partial u$ denotes the mechanical to electrical coupling.

Consider first the calculation of the right hand side vector in Equation (23). The mechanical and electrical residuals, the deformation coefficient matrix and the transformation matrix (setup phase) of the precorrected FFT algorithm are computed in the outer Newton loop. The deformation coefficient matrix is stored in sparse ordered and factored form. A sparse solver is then employed to compute $R_{Mu}^{-1}R_M$. $R_{Eq}^{-1}R_E$ is computed by employing the GMRES algorithm. The matrix-vector product needed in the GMRES algorithm is computed by employing the evaluation pass of the precorrected FFT algorithm. Note that no setup phases are needed inside the GMRES algorithm. Next, consider the computation of $R_{Mu}^{-1}R_{Mq}\Delta q^{(i)}$ and $R_{Eq}^{-1}R_{Eu}\Delta u^{(i)}$ required in the inner GMRES loop. Denoting $v_1^{(j)}$ and $v_2^{(j)}$ to be the jth iteration GMRES approximations to $\Delta u^{(i)}$ and $\Delta q^{(i)}$, respectively, $R_{Mq}v_2^{(j)}$ and $R_{Eu}v_1^{(j)}$ are first computed. A sparse solve is then employed to compute $R_{Mu}^{-1}R_{Mq}v_2^{(j)}$ and a GMRES solver to compute $R_{Eq}^{-1}R_{Eu}v_1^{(j)}$. The preconditioned Newton-GMRES algorithm is briefly summarized in Algorithm 2.

Algorithm 2: Preconditioned Newton-GMRES technique

while not converged /* outer Newton loop */
  compute R_M, R_E
  compute transformation matrices for precorrected FFT
  compute and factor R_{Mu}
  sparse solve to obtain $R_{Mu}^{-1}R_M$
  use GMRES to compute $R_{Eq}^{-1}R_E$
  while not converged /* inner GMRES loop */
    /* steps to compute matrix-vector product in
      jth gmres iteration */
    compute $R_{Mq}v_2^{(j)}$
    sparse solve to obtain $R_{Mu}^{-1}R_{Mq}v_2^{(j)}$
    compute $R_{Eu}v_1^{(j)}$
    use GMRES to compute $R_{Eq}^{-1}R_{Eu}v_1^{(j)}$

    /* remaining steps of gmres not shown */

  end while
  update u
  update q
end while

V. Results

Numerical results are presented for two examples: a beam over a ground plane structure and a comb drive structure. The performance of coupled and relaxation algorithms is examined for both

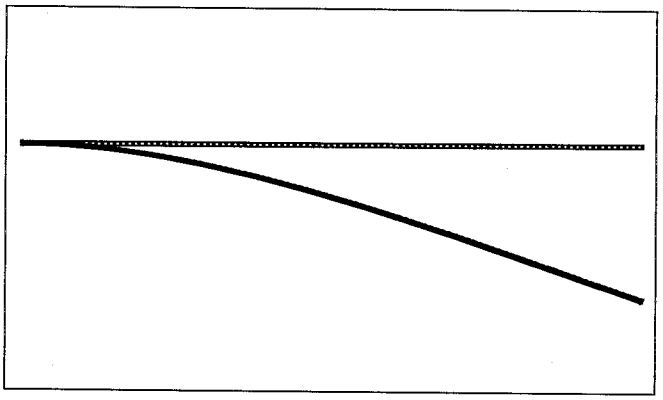

Figure 3. Deflection of the beam for an applied bias of 2.38 V.

examples on a Dec alpha workstation. In particular, the convergence characteristics and the simulation times are compared.

The beam structure considered is 80 μm long, 10 μm wide, 0.5 μm thick, and is positioned 0.7 μm above the ground plane. When a positive potential with reference to the ground plane is applied on the beam, the beam deflects towards the ground plane because of the electrostatic force. As the potential difference increases, the tip of the beam approaches the ground plane, and touches the ground plane for a certain bias defined as the pull-in voltage. The pull-in voltage for the beam considered here is 2.39 V. The deflection (not to scale) of the beam at 2.38 V is shown in Figure 3.

The comparison of relaxation and coupled algorithms for the entire bias sweep is summarized in Table I. As the bias approaches the pull-in value, the relaxation algorithm requires more iterations to converge. This is due to the increased coupling between elastostatic and electrostatic equations and the relaxation algorithm converges more slowly or fails to converge in the tightly coupled case. Comparison of the simulation times reveals that the coupled algorithm is competitive with the relaxation algorithm when the relaxation algorithm converges rapidly (see e.g the simulation times for an applied bias of 1.0 V). For an applied bias larger than 1.0 V, the coupled algorithm is very efficient and runs much faster compared to the relaxation algorithm. To predict the pull-in voltage for the beam structure, the relaxation algorithm takes a total of 91285.9 seconds while the coupled algorithm takes 42885.8 seconds. So the coupled algorithm is about 2.13 times faster than the relaxation algorithm for this example. We have obtained greater speedups for other devices. A comparison of the convergence behavior of relaxation and coupled algorithms for an applied bias of 2.38 V is shown in Figure 4.

TABLE I

COMPARISON OF RELAXATION AND COUPLED ALGORITHMS FOR NUMBER OF ITERATIONS AND CPU(SEC) FOR A BEAM AND GROUND PLANE EXAMPLE

Bias	# Iterations		CPU(sec)	
	Relaxation	Coupled	Relaxation	Coupled
1.0	6	3	3511.4	3768.4
1.5	8	3	4753.5	4070.6
2.0	13	4	7693.5	5251.7
2.25	20	6	11756.6	9096.9
2.35	36	6	20821.9	8953.8
2.38	75	7	42749.0	11744.4

The comb example consists of a deformable comb structure, a drive structure and a ground plane. When a positive potential is applied on the drive structure, and zero potential on the comb and the ground plane, the comb structure deforms out of plane. The

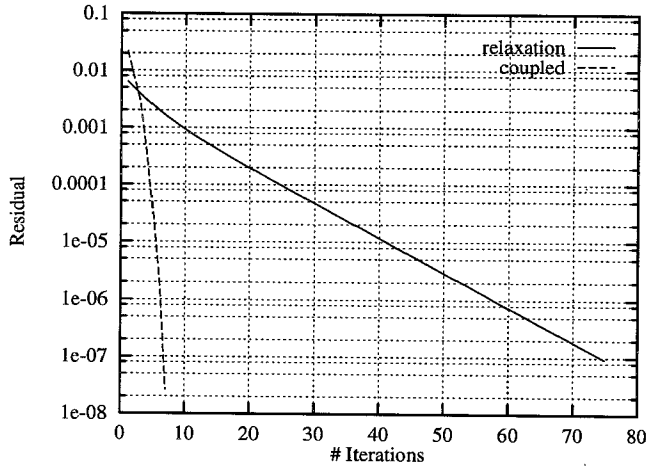

Figure 4. Comparison of convergence of relaxation and coupled algorithms just before pull-in for the beam and ground-plane example

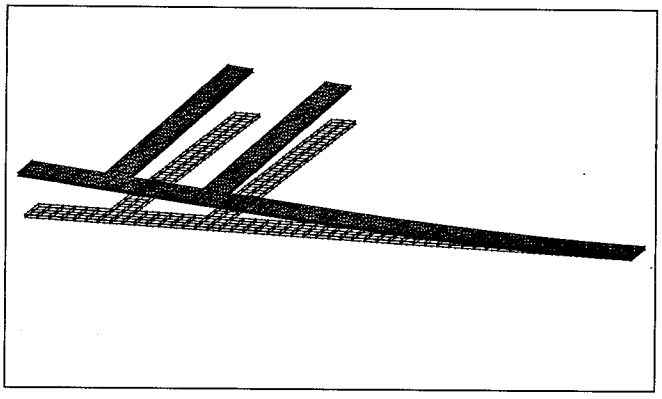

Figure 5. Deflection of the comb for an applied bias of 85 V.

deformation (not to scale) of the comb structure for an applied bias of 85 V is shown in Figure 5. Note that only the deformation of the comb structure is shown as the drive and the ground plane do not move.

TABLE II

COMPARISON OF RELAXATION AND COUPLED ALGORITHMS FOR NUMBER OF ITERATIONS AND CPU(SEC) FOR A COMB DRIVE EXAMPLE (A * INDICATES THAT THE ALGORITHM FAILS TO CONVERGE FOR THE BIAS)

Bias	# Iterations		CPU(sec)	
	Relaxation	Coupled	Relaxation	Coupled
25.0	7	6	3595.4	5589.8
50.0	16	8	9138.0	11833.5
75.0	70	10	42160.3	18590.7
80.0	142	9	81827.0	16670.2
85.0	*	10	*	18490.9

A comparison of the relaxation and coupled algorithms for the comb example is summarized in Table II. At low voltages, the deflection of the comb is small, the coupling between the electrical and mechanical systems is weak and the relaxation algorithm works very well. At low voltages, the coupled algorithm takes half as many iterations as the relaxation algorithm and the simulation time for the coupled algorithm is a little longer. For higher voltages, the coupled algorithm converges much faster compared to the relaxation

algorithm. For a bias of 80 volts, the coupled algorithm is about 3.8 times faster. The convergence of the relaxation and coupled algorithms at 80 V bias is shown in Figure 6. For an application

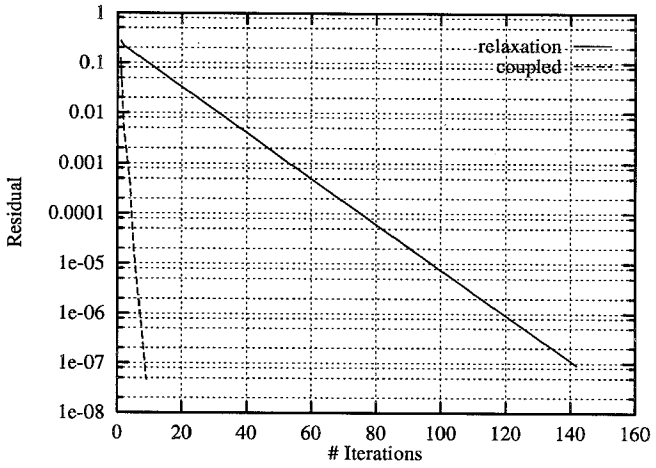

Figure 6. Comparison of convergence of relaxation and coupled algorithms for a comb example at an applied bias of 80 V.

of 85 V on the drive, the relaxation algorithm fails to converge. The coupled algorithm converges very rapidly and takes only 12 iterations. This is illustrated in Figure 7.

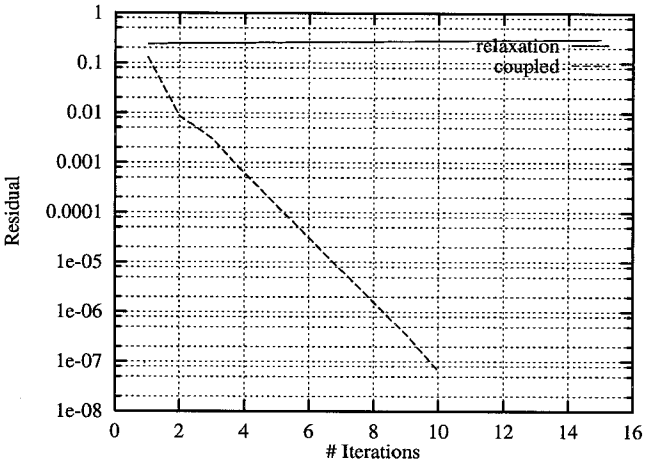

Figure 7. Comparison of convergence of relaxation and coupled algorithms for a comb example at an applied bias of 85 V.

VI. Conclusion and Acknowledgements

In this paper, we presented a coupled algorithm for 3-D electromechanical analysis. The coupled algorithm employs a Galerkin finite-element method for the elastostatic analysis and a boundary-element method with precorrected FFT acceleration for the electrostatic analysis. The mechanical to electrical coupling term is computed by direct integration and a matrix-free technique is employed to compute the electrical to mechanical coupling term. A block diagonal preconditioner is applied to accelerate the convergence of the GMRES algorithm. Numerical results presented for 3-D electromechanical structures show that the coupled algorithm converges rapidly and is much faster as compared to the relaxation algorithm. Convergence of the coupled algorithm is demonstrated for a comb drive example for which the relaxation algorithm fails to converge.

The authors would like to thank Dr. John R. Gilbert, Dr. Peter M. Osterberg, Joel R. Phillips and Professor Steven D. Senturia for many valuable discussions.

References

[1] N. R. Aluru and J. White, "Direct-Newton finite-element/boundary-element technique for micro-electromechanical analysis," *Technical Digest IEEE Solid-State Sensor and Actuator Workshop*, Hilton Head Island, SC, June 1996.

[2] M. Bachtold, J. G. Korvink, J. Funk and H. Baltes, "New convergence scheme for self-consistent electromechanical analysis of iMEMS," *Proc. IEDM 1995.*

[3] K. J. Bathe, E. Ramm and E. L. Wilson, "Finite element formulation for large deformation dynamic analysis,"*Int. J. Num. Meth. Engrg.*, vol. 9, pp. 353-386, 1975.

[4] A. Brandt, "Multilevel computations of integral transforms and particle interactions with oscillatory kernals," *Computer Physics Communications*, no. 65, pp. 24–38, 1991.

[5] X. Cai, H. Yie, P. Osterberg, J. Gilbert, S. Senturia and J. White, "A relaxation/multipole-accelerated scheme for self-consistent electromechanical analysis of complex 3-D microelectromechanical structures," *Proc. ICCAD 1993.*

[6] J. R. Gilbert, R. Legtenberg and S. D. Senturia, "3D coupled electromechanics for MEMS: Applications of CoSolve-EM," *Proc. MEMS 1995.*

[7] P. E. Gill, W. Murray and M. H. Wright, *Practical Optimization*, Academic Press, London, 1981.

[8] L. Greengard, *The Rapid Evolution of Potential Fields in Particle Systems*. Cambridge, MA: M.I.T. Press, 1988.

[9] J. L. Hess and A. M. O. Smith, "Calculation of potential flow about arbitrary bodies," *Progress in Aero. Sci.,* vol. 8, pp. 1-138, 1966.

[10] Hibbit, Karlsson and Sorenson, Inc., Providence, R.I.

[11] K. S. Kundert and A. Vincentelli, "Sparse User's Guide: A sparse linear equation solver," *Univ. of California, Berkeley*, 1988.

[12] L. E. Malvern, *Introduction to the Mechanics of Continuum Medium,* Prentice-Hall, Englewood Cliffs, N.J., 1969.

[13] K. Nabors and J. White, "FastCap: A multipole-accelerated 3-D capacitance extraction program," *IEEE Trans. CAD*, vol. 10, pp. 1447-1459, 1991.

[14] J. R. Phillips and J. White, "A Precorrected-FFT method for capacitance extraction of complicated 3-D structures," *Proc. ICCAD 1994.*

[15] S. Rao, T. Sarkar and R. Harrington, "The electrostatic field of conducting bodies in multiple dielectric media," *IEEE Trans. Microwave Theory Tech.*, vol. MTT-32, pp. 1441-1448, Nov. 1984.

[16] A. Ruehli and P. A. Brennen, "Efficient capacitance calculations for three-dimensional multiconductor systems," *IEEE Trans. Microwave Theory Tech.*, vol. MTT-21, pp. 76-82, Feb. 1973.

[17] Y. Saad and M. H. Schultz, "GMRES: A generalized minimal residual algorithm for solving nonsymmetric linear systems," *SIAM J. Sci. Stat. Comput.*, vol. 7, pp. 856-869, 1986.

[18] H. U. Schwarzenbach, J. G. Korvink, M. Roos, G. Sartoris, and E. Anderheggen, "A microelectromechanical CAD extension for SESES," *JMEMS*, vol. 3, pp. 162-171, 1994.

[19] H. Yie, X. Cai and J. White, "Convergence properties of relaxation versus the surface-Newton generalized-conjugate residual algorithm for self-consistent electromechanical analysis of 3-D MEMS" *Proc. NUPAD V 1994.*